Advances in Bioresearch
Adv. Biores., Vol 15 (5) September 2024:77-93

Print ISSN 0976-4585; Online ISSN 2277-1573
Journal's URL:http://www.soeagra.com/abr.html
CODEN: ABRDC3
DOI: 10.15515/abr.0976-4585.15.5.7793

Advances in Bioresearch

ORIGINAL ARTICLE

Optimization of Saxagliptin Liquisolid Tablet: Augmenting Dissolution and Oral Therapeutic Efficacy for Diabetes Management

Mohan Dhere[1], Bhavya E[2]*, Satheshkumar Sukumaran[3], Sunil Galatage[4], Arehalli Manjappa[4] and Sameer Nadaf [5]

[1]Department of Pharmacy, Vels Institute of Science, Technology and Advanced Studies (VISTAS), Pallvaram, Chennai, INDIA.

[2*]Department of Pharmacy Practice, Saveetha College of Pharmacy, Saveetha Institute of Medical and Technical Sciences, Thandalam, Chennai, INDIA.

[3]Department of Pharmaceutics Vels Institute of Science, Technology and Advanced Studies (VISTAS), Pallvaram, Chennai, Tamil Nadu, INDIA.

[4]Department of Pharmaceutics, Vasantidevi Patil Institute of Pharmacy, Kodoli, Kolhapur, Maharashtra, INDIA.

[5] Department of Pharmaceutics Bharati Vidyapeeth College of Pharmacy, Palus, Sangli, Maharashtra, INDIA.

*Corresponding Author Email: bhavyae.scop@saveetha.com

ABSTRACT

Saxagliptin, a dipeptidyl peptidase-4 (DPP-4) inhibitor, is broadly used in the management of type II diabetes mellitus due to its ability to improve glycemic control by inhibiting the degradation of incretin hormones. However, its therapeutic efficacy is limited by its poor aqueous solubility, leading to insufficient dissolution and reduced bioavailability. To address this challenge, this research aimed to devise a liquisolid tablet (LST) formulation incorporating saxagliptin (SGN-LST) to enhance its dissolution rate and therapeutic efficacy against diabetes. Employing a 3^2-full factorial design, we optimized the SGN-LST formulation by investigating the carrier-to-coating ratio and the ratio of neusilin-US2 to corn starch. Neusilin-US2 was utilized to convert the saxagliptin liquisolid formulation into solid, easily manageable granules. The optimized SGN-LST underwent comprehensive characterization for drug content, crystallinity via X-ray diffractometry, drug release kinetics, in vitro antidiabetic potential, and in vivo pharmacokinetic behavior. FTIR spectral analysis indicated no compatibility issues, while DSC and XRD analyses affirmed the amorphous nature and homogeneous dispersion of SGN within the liquisolid tablet matrix. Among the formulations tested, SGN-LST-6 (comprising maisine with a neusilin to corn starch ratio of 8:2) exhibited rapid disintegration (56.15±2.14 sec) and high cumulative drug release (98.76±2.88%). Notably, SGN-LST-6 demonstrated significant α-amylase and α-glucosidase inhibitory activity compared to plain SGN and conventional acarbose ($P<0.05$), signifying potent antidiabetic effects. Furthermore, oral administration of optimized SGN-LST yielded a four-fold rise in bioavailability in rats in contrast to plain SGN. This study demonstrates the remarkable improvement of both in vitro and in vivo efficacy of SGN in diabetes treatment through the development of SGN-LST. These findings suggest that liquisolid tablets could serve as an efficacious delivery system for SGN in the management of diabetes.

Keywords: *Sexagliptin, Maisine, Liquisolid tablet, Anti-diabetic, Oral pharmacokinetics.*

Received 14.04.2024 Revised 23.05.2024 Accepted 24.07.2024

How to cite this article:
Mohan D, Bhavya E, Satheshkumar S, Sunil G, Arehalli M and Sameer N. Optimization of Saxagliptin Liquisolid Tablet: Augmenting Dissolution and Oral Therapeutic Efficacy for Diabetes Management. Adv. Biores. Vol 15 [5] September 2024. 77-93

INTRODUCTION

A partial or total absence of insulin induces hyperglycemia, a chronic illness known as diabetes mellitus (DM), which has both immediate and long-term effects [1]. 422 million people worldwide suffer from

diabetes, most of whom reside in low as well as middle-income nations. The disease also claims 1.5 million lives each year. Consequently, during the last few decades, there has been a progressive increase in both the incidence and prevalence of diabetes [2]. Diabetes considerably increases the risk of having renal failure, coronary heart disease, and blindness [3]. The oral method of medication delivery is favored over alternative routes owing to its ease of administration, more affordable, and more widely accepted by patients. Upon dissolving in the gastrointestinal tract (GIT), medications taken orally are absorbed into the bloodstream. Therefore, for oral medications with low water solubility, dissolution is assumed to be a critical factor in determining the rate of absorption [4]. Due to poor water solubility and restricted intestinal permeability, 40% of recently produced medications present substantial biopharmaceutical problems that ultimately result in poor drug absorption and submaximal therapeutic effect [5]. Saxagliptin (SGN), a new oral hypoglycemic medicine, is a member of the DPP-4 inhibitor class [6]. It is widely accepted because of its moderate dosage and little danger of weight gain. It has also been used as a supplement to other anti-diabetic medications and lifestyle changes to target glycemic control [7]. Although SGN has excellent anti-diabetic potential, its use is constrained due to its insufficient solubility in aqueous solutions, which prevents the complete dose from dissolving in the digestive system resulting in poor oral bioavailability [8]. The above facts of SGN necessitate their delivery using a novel approach to improve oral bioavailability and therapeutic effectiveness in the treatment of DM. For increasing the solubility of pharmaceuticals in water, several technological advancements have been investigated including solid dispersion [9]. crystal engineering [10]. Micronization [11]. mesoporous carriers, etc. Liquisolid compact compositions are currently showing intriguing promise of improving the dissolution capability and oral bioavailability of the therapeutics [12-14]. In this technique, the carrier, as well as coating material, are utilized to dissolve the medications into solids that can be efficiently compressed into liquisolid compacts. The medicine is more easily dissolved and loaded onto the carrier with the aid of the non-volatile solvent. Liquisolid compacts make it easier for the medicine to be wetted and dissolved more quickly, boosting oral bioavailability attributes. Liquisolid tablets are made using powder compacts that allow for the loading of medicines into their adsorbed liquid form. The liquisolid technique utilizes a simple physiological blending process with specific excipients known as the carrier and coating material to transform a liquid into a free-flowing, easily compressible, and dry powder. Liquisolid systems are easily developed with low cost, ease, and quick process along with scale-up [15]. Lately, a lot of lipophilic and poorly water-soluble medications or plants, like Curcuma comosa [15]. telmisartan [16]. lovastatin [17]. chlorpromazine [18]. Glyburide [19]. Glimepiride [20]. Rosuvastatin [21]. Fenofibrate [22]. etc. have been formulated into liquisolid compact to escalate their oral bioavailability and the therapeutic efficacy. Thus, a liquisolid tablet can potentially augment the dissolution rate and oral bioavailability of SGN. Therefore, the current study concentrated on using the liquisolid compact technology to increase the dissolution rate as well as the therapeutic effectiveness of SGN. The liquisolid compacts were designed and optimized via 3^2 factorial designs. Different characteristics, including flowability, crystallinity, in vitro drug release, etc., were assessed for the optimized liquisolid tablet. Additionally, the in vivo pharmacokinetic efficacy in rats and the in vitro antidiabetic potential of the improved formulation has been investigated.

MATERIAL AND METHODS

Materials

Saxagliptin was purchased from Aditya Imptex Pvt. Ltd., Mumbai, India. We received free samples of Maisine, Labrasol, Kolliphor, Kollisolv, and Cremophor-RH-40 from Gattefosse in Mumbai, India. A sample of Neusilin-US2 has been kindly supplied by Fuji Chemicals, Japan as a gift. From Unique Chemicals in Kolhapur, India, we bought double-distilled water, Tween 20, Tween 80, and PEG 400. Analytical-grade chemicals have been used in this study.

Screening of suitable lipid through drug solubility study

The solubility experiment was carried out using the phase solubility technique. In short, 2 mL of each of the various lipids were added to each test tube, along with an excessive amount of SGN. The resulting mixes were agitated using an orbital shaker for 24 h at 37°C (Remi-24 Plus, India). Following balance, each sample was centrifuged for 15 min at 2000 rpm employing a Remi-India RM-12C centrifuge. A UV visible spectrophotometer (Shimadzu-1900, Japan) was employed to measure the absorbance values at 211 nm after the clear supernatant was filtered by a membrane having a porous size of 0.45 micrometers [23].

Method for formulating liquisolid tablet

The SGN along with non-volatile co-solvent were transferred to a 20mL glass beaker in the prescribed amounts. After that, the beaker was heated gradually until all of the SGN had become soluble. To attain a

uniform distribution of the liquid medication in the powder, the resulting heated liquid medication was combined with the powder excipient for nearly a minute at an assessed mixing rate of one rotation per second. The initial specified amount of carrier and coating components were then combined with the resultant warm liquid medicine. Further, liquid/powder admixture was homogeneously spread over a mortar's surface and then let to stand for around 5min to allow the medication solution to permeate the powder's internal matrix. In addition, the powder is removed from the mortar's surface utilizing an aluminum spatula before being combined with the disintegrating agent for a further 30 sec in the manner previously indicated. The final liquisolid mixture produced was then compressed into tablets [24].

Application of Mathematical model for designing SGN liquisolid tablet

By using a mathematical model, Bolton, and Spireas were able to produce liquisolid tablets with the right compatibility and flowability. This model is based on the idea that, while maintaining adequate flowability and compatibility, the interior matrix of a powder substance can only store so much liquid medicine (co-solvent+drug). The flow behavior and "the powder material compatibility begins to deteriorate as the fraction of liquid crosses a predetermined threshold. The highest liquid quantities that a powder material may retain though still retaining acceptable flowability and compatibility are the (Φ-number) flowable liquid-retention potential and (Ψ-number) compressible liquid-retention potential. Acceptable compatibility is the capacity of a powder material to form cylindrical compacts with acceptable friability and crushing strengths (about 5-6kg/cm^2) without exhibiting any "liquid-squeezing-out" phenomenon. The liquid medication is infused into the inner matrix" until it is fully saturated, the extra liquid starts to build up like a coating on a powder material's surface. In addition to the extra powder excipients, referred to as "coating material," the extra liquid layer is eventually absorbed, leaving the overall free-flowing powder material, compressible, and non-adherent. The "excipient ratio" (R) "is the proportion of carrier to coating material necessary to generate powder by the required compressibility and flowability [16].

$R = Q/q$ Eq. (1)

Here q is the amount of coating material and Q is the amount of carrier material.

Determination of flowable liquid retention potential (Φ - value)

10 g of powder was added to the liquid formulation gradually, and the" resulting mixture was then put on a polished metal plate at one end. One side of the metal plate has risen gradually off the surface while leaving the ground on the other side. The slip angle was defined as the angle that occurs between the plate and the ground.[25] The ideal flowability attribute of a powder excipient for the particular liquid vehicle used is a sliding angle value of approximately 33º.

Determination of compressible liquid retention potential (Ψ- value)

To create a homogeneous admixture, 1 g of powder is homogeneously mixed with the liquid medication. To create a tablet, the mixture was squeezed in the rotating tablet machine to a certain hardness. The hardness range between 5 to 7 Kg was deemed appropriate in this experiment. Additionally, it was noted that no liquid medication leaked during compression through the powder admixture [26].

Liquid load factor

After determining the "Φ-value and Ψ-value of the carrier and coating material, the load factor of liquid was computed using the following formulas for acceptable flowability and compressibility.

$$\Phi Lf = \Phi CA + \Phi CO \left[\frac{1}{R}\right] - \text{flowability} \qquad \text{Eq. (2)}$$

$$\Psi Lf = \Psi CA + \Psi CO \left[\frac{1}{R}\right] - \text{compressibility} \quad \text{Eq. (3)}$$

Here, ΦCA and ΦCO represent the carrier and coating materials' respective flowability and compressibility liquid retention potentials. ΨCA and ΨCO also stand for the same materials' combined flowability and compressibility liquid retention potentials. According to Eq (1), R represents the excipient ratio. The R-value between 10 and 20 was shown to produce the best flow properties and acceptable compatibility properties in investigations that were reported in various research journals, consequently, in this study's calculation; a mean of 15 has been used [27]. The liquid load factor was computed by applying a formula using the liquid and the carrier material weights.

$$Q = \frac{W}{Lf} \quad \text{Eq. (4)}$$

Q = Carrier material weight and W = Liquid medicament weight.

Whichever had the lower value between Φ Lf and Ψ Lf was included in the equation (4). The carrier material weight needed to ingest a specific liquid medication was provided by Eq. (4). The Q is the

obtained value that has been used by Eq. (1) to estimate the coating material value necessary to remove the additional layer of liquid through the surface.

Primary trial for selection of carrier and coating material

Finding the coating and carrier materials that can carry the most liquid medication without sacrificing flowability and compatibility was the initial goal of the research. The screening methods are defined in the aforementioned section under the headings Determination of flowable liquid retention potential and Determination of compressible liquid retention potential. The attained data were utilized to calculate the liquid loading factor in Eqs. (3) and (4).

Optimization of SGN-liquisolid tablet (SGN-LST) by factorial design

The Design Expert program utilized 3^2 full factorial designs to optimize the SGN-liquisolid tablet. 3 levels per independent variable-high (+1), medium (-1), and low (-1)-were examined in the association between two independent factors, carrier: coating ratio (X_1) and neusilin: corn starch ratio (X_2), and two dependent variables, drug release (Y_1) and disintegration time (Y_2). Table 1 displays the nine trial runs that the Design Expert software generated using the levels. The approach was followed in developing all formulations, and the dependent or response variables of drug release (Y_1) and disintegration time (Y_2) were evaluated. Two-factor and linear interactions are terms utilized to define a variety of mathematical models. ANOVA was employed to eliminate the responses that were employed to evaluate the statistical significance of the developed model and its terms. In order to examine the relationship and correlation between the dependent, independent, and other response variables, the Design Expert® program generated 2D, 3D, and perturbation graphs. Lastly, utilizing numerical and graphical optimization techniques, the necessary formulation SGN-LST was refined according to characteristics like reduced disintegration time and percent cumulative drug release [28].

Table 1. Full factorial Design matrix summarizing the levels, factors, and responses of 09 runs for optimization of SGN liquisolid tablet (SGN-LST).

Run	Block	Factor 1 Carrier: Coating Ratio	Factor 2 (X2) (Neusilin: Corn starch Ratio) (R value)	% Cumulative Drug Release (Y1)	Disintegration Time in Sec (Y2)
1	SGN LST-1	5 (-1)	9:1 (-1)	63.43±4.32	78.12±6.54
2	SGN LST-2	10 (0)	9:1 (-1)	69.12±3.32	74.43±5.32
3	SGN LST-3	15 (1)	9:1 (-1)	74.32±4.87	71.52±3.65
4	SGN LST-4	5 (-1)	8:2 (0)	82.65±2.12	67.32±4.73
5	SGN LST-5	10 (0)	8:2 (0)	91.67±2.82	62.71±3.28
6	SGN LST-6	15 (1)	8:2 (0)	98.76±2.88	56.15±2.14
7	SGN LST-7	5 (-1)	7:3 (1)	84.65±3.65	60.45±3.43
8	SGN LST-8	10 (0)	7:3 (1)	87.42±3.43	55.08±2.54
9	SGN LST-9	15 (1)	7:3 (1)	91.23±2.34	52.82±1.72

Factor	**Levels used, actual (coded)**		
	Low (-1)	Medium (0)	High (+1)
Independent variables			
Factor 1 (X_1) (Carrier: Coating Ratio)	5	10	15
Factor 2 (X_2) (Neusilin: Corn starch ratio)	9:1	8:2	7:3
Dependent variables			
Drug Release (Y_1)	**Maximize**		
Disintegration Time (Y_2)	**Minimize**		

Micrometric properties of optimized batch

Bulk Density (BD) and Tapped Density (TD)

The initial volume (Vb) of SGN liquisolid tablet powder of Weight 'W' (n = 3) was measured after it was placed into a graduated cylinder (100mL). Following that, the sample was tapped until constant volume (Vt) was reached using a bulk density apparatus (Lab Hospital, Mumbai, India). We computed the TD and BD using the following formulas [29].

$$BD = \frac{W}{Vb} \qquad \text{Eq. (5)}$$

$$TD = \frac{W}{Vt} \qquad \text{Eq. (6)}$$

Carr's Index (CCI) and Hausner's ratio (HR)

The findings of TD and BD were employed for the calculation of CCI and HR. CCI and HR were evaluated in triplicates as follows,

$$CCI = \frac{(TD - BD)}{(TD)} \times 100 \quad \text{Eq. (7)}$$

$$HR = \frac{(TD)}{(BD)} \quad \text{Eq. (8)}$$

Angle of Repose (θ)

The angle of repose was estimated by employing a fixed-funnel approach. Simply, SGN liquid-solid tablet powder was funneled into a pile whose height "H" and radius "R" were measured. The formula used to get the angle of repose is shown below [30].

$$\theta = Tan^{-1}\left(\frac{H}{R}\right) \quad \text{Eq. (9)}$$

Post-compression evaluation

Hardness

By utilizing a Monsanto hardness tester, the tablets' hardness of six tablets was assessed.

Friability Test

The test had been carried out using the Roche friabilator (Electro lab). Weighted (W_0) 6.5 gm of tablets were added to the friabilator, which was then rotated for 4 min at a speed of 25 rpm. The tablets were gathered, cleaned, and weighed once more. The percentage of friability was calculated using the weight (W_t) differential between the initial and final weights.

Weight Variation Test

20 tablets were chosen at random, and each one was weighed separately. Three samples' average weights and standard deviations (SD) were computed. The weight of tablets that were deemed to have passed weight had an average weight deviation of not more than 2.5% for any one tablet and no more than 5% for any other tablet [31].

Drug Content

The 10 SGN liquisolid tablets were weighed precisely, crushed, the right quantity of methanol was added, and then scattered. The material was examined spectrophotometrically at 211nm utilizing a filter having 0.45µm pore size after removing the clear supernatant with the help of Shimadzu UV-1900 [32].

In Vitro Disintegration Time

Using a disk-shaped disintegration test instrument (Electrolab, India), the time of disintegration for all SGN liquisolid tablets was computed in the 900mL distilled water at a temperature of (37±2°C) at the rate of 30±2 cycles/min [33].

In Vitro Drug Release Study

All SGN liquisolid tablets were subjected to an *in vitro* drug release investigation utilizing USP type II equipment (EDT-08Lx Electro lab) at a temperature of 37±0.5°C, 50 rpm, and 0.1N HCl as a dissolution media. At the specified time intervals (15, 30, 45, and 60 min.), samples of 5mL had been removed and changed with the new dissolving solution. Withdrawn samples were diluted, passed through a filter of a membrane (0.45 µm), and then analyzed at 211nm with a UV-spectrophotometer (Shimadzu-1900) [34].

Drug excipient compatibility study

Fourier transforms infrared (FTIR) spectroscopy

The FTIR spectra of pure SGN, maisine, neusilin-US2, and the optimized SGN liquisolid tablet were noted employing a Bruker Alpha-T FT-IR spectrophotometer, covering a frequency range of 4000-650 cm^{-1} [35].

Differential scanning calorimetry (DSC)

The DSC thermograms of pure SGN, maisine, neusilin-US2, and the upgraded SGN liquisolid tablet (Shimadzu, Japan) have been evaluated utilizing a DSC-60 calorimeter. Onto the metal pans, the precisely weighed sample was added before being sealed. Over the complete temperature range, the sample was heated at a rate of 10°C/min from 0°C - 400 °C [36].

P-XRD diffraction (XRD)

The crystalline features of SGN, "Neusilin-US2, and the revised formulation were assessed with an X-ray diffractometer (Philips- diffractometer, Netherlands). The samples had been scanned at 2θ values between 10° and 80° [37]

***In vitro* antidiabetic study**

α-amylase inhibitory assay

An Eppendorf tube was filled with PBS solution" (1 mL), and 0.5 mL of samples at different conc. (50 to 250 µg/mL), and 200 µL of 0.5mg/mL α-amylase and 5mg/mL starch solution. After that, the mixture was

kept undisturbed at room temperature for 10 min. Starch with and without amylase was used as the control. After stopping the reaction mixture with 400 µL of dextrose and sodium chloride (DNS) solution, the mixture was heated for 05 min in a water bath before cooling. At 540 nm, the absorbance was computed (Labman UV-Visible Spectrophotometer) and % enzyme inhibition was "determined. [38-39]
% of α-amylase inhibition = [(Ac−As)/Ac] ×100 eq. (10). here, As and Ac as absorbance of sample" and control, correspondingly.

α-Glucosidase inhibition assay

In brief, a 50 mM 6.5 PBS solution was utilized to dissolve ρ-Nitrophenyl-ρ-D-glucopyranoside (PNPG). By using serial dilution, a method sample of different conc. (50 to 250µg/mL) were prepared in a 5 percent DMSO solution. 30µL of each conc. was added with 36 µL 6.8 PBS solution and 17 µL 5mM PNPG. The mixed solution had been incubated at 37°C for 5 min. After the initial incubation, 17 µL of -glucosidase was added to this solution, and it was then incubated once more for 15 min at 37°C. To terminate the enzymatic reaction after the second incubation, 100µL "of Na_2CO_3 267 mM was transferred to the solution. Using a microplate reader, solution absorbance was measured" at 405nm [40].

***In vivo* pharmacokinetic study**

IAEC (The Institutional Animal Ethics Committee) of the BIRD, Sangli has given its approval to the study's experimental procedure (BIRD/CPCSEA/IAEC/Sangli/2022-23/06). Wistar albino rats (n=9) from Crystal Biological Solution in Pune, India, weighed between 180 and 220 g were used for the study. Before the trial, the animals were fed a typical enriched meal and given access to water for two weeks. The rat population was divided into three groups at random. Group I acted as the control group, while groups II and III had been chosen as the test and standard groups. Group I received a physiological saline solution. While group III received SGN dispersed in 0.5 percent sodium carboxymethyl cellulose at a dose of 5mg/kg, group II animals received optimal SLT at an equivalent dosage of SGN (5mg/kg). 500µL of blood were extracted from the retro-orbital plexus of each rat after the dosage injection, and the tubes were filled with heparinized polyethylene at regular intervals (0.5, 1, 2, 4, 6, 8, 10, 12 and 24 hours). Blood samples were obtained, and the plasma was centrifuged for 10 min at 7000 rpm. It has been frozen at a temperature of -20°C. The concentrations of SGN in the isolated samples of plasma were determined using the validated RP-HPLC technique. The different pharmacokinetic parameters such as the T_{max} (time required to achieve C_{max}), "C_{max} (maximum plasma concentration), $AUMC_{0-\infty}$ (area under the moment curve), $AUMC_{0-\infty}$ (area under the moment curve), and MRT (Mean Residence Time) were investigated [23].

Stability study

A stability study was conducted for 90 days by ICH guidelines at 40±2°C and 75±5% RH. At certain intervals, several" metrics including cumulative drug release (%CDR) and drug content (%) have been measured by following 1, 2, and 3 months, respectively [41].

RESULTS

Screening of lipids using solubility studies

To choose the best vehicle that might solubilize the SGN in maximum quantity, the solubility of the SGN was estimated. SGN solubility in lipids has been discovered 5.43±1.54 to 38.54±3.78 mg/mL. Maisine has the highest solubility (38.54±3.78 mg/mL). Table 2 displays comprehensive findings from solubility investigations.

Table 2. Solubility of Saxagliptin in Lipids.

Lipid and surfactant	Solubility (mg/mL) *
Maisine	38.54±3.78
Labrasol	17.12±0.2.34
Propylene Glycol	15.54±1.12
PEG-400	22.16±4.64
Kolliphor	8.16±2.87
Kollisolv	5.43±1.54
Cremophor RH40	7.44±2.52
Tween 20	6.94±2.21
Tween 80	8.72 ±1.57

***Each value represents mean ± SD of three observations**

Mathematical Modeling

Determination of flowable liquid-retention potential

Neusilin had the highest value, 1.5 mL, of all the examined carrier materials. This indicated that neusilin powder of 1 gm may be mixed with 1.5 mL of liquid medication and retain its potent flow properties

(angle of slide=31). Neusilin was chosen as the carrier material because neusilin-US2 has been associated with compressil 101, fujicalin, and microcrystalline cellulose, in that order [15]. Aerosil has the largest flowable liquid retention potential of any coating material evaluated, with a capacity of 1.8 mL. Initial dissolution investigations revealed that the liquisolid tablet with simply neusilin as the carrier material has been unable to completely release the medication. This may have happened as a result of the SGN being tightly confined inside the neusilin internal matrix. To address this problem, maize starch has been combined with the neusilin. Starch is commonly utilized in tablets as a dissolving agent owing to its capacity to swell. It was anticipated that the starch's ability to expand would make it easier for the medicine to release from neusilin's large interior surface area.[42] For three freshly made combinations of neusilin-US2 and maize starch with ratios of 1:9, 2:8, and 3:7, the angle of the slide was calculated. Practical observations revealed that the liquid retention capability of corn starch and neusilin in the ratios of 1:9, 2:8, and 3:7 was identical to that of plain neusilin (1.5 mL). The liquid retention potential began to substantially drop in the succeeding trials as the maize starch proportion in the given mixture was further raised, hence it has been determined to employ Neusilin/cornstarch mixture like the carrier material in ratios of 1:9, 2:8 and 3:7.

Determination of compressible liquid-retention potential

Neusilin-US2 and maize starch were found to interact in the compressibility test in the ratios of 1:9, 2:8, and 3:7 and were able to give a satisfactory hardness and hold 1.5 mL of maisine without experiencing any leaking issues.

Liquid load factor

Using Eqs. (2) and (3), the liquid load factor was computed. For Neusilin/corn starch (9:1, 8:2, and 7:3), the U-value and W-value were discovered to be 1.5mL, as previously demonstrated. The aerosil 200 coating material's U-value for the chosen coating was 1.8 [26]. The R-value of 15 was used, as indicated in the introduction [42,43]. The values of U-Lf and W-Lf were 1.8 and 1.5, respectively. The value of W-Lf was ultimately taken into consideration as a liquid load factor for this specific liquisolid system since the W-Lf < U-Lf.

Determination of the weight of liquid medication

SGN was shown to dissolve in maisine at a practical solubility of 38.54 mg/mL. The total weight of the liquid medication was 269.47 mg because it took 259.47 mg of maisine to dissolve 10 mg of SGN (Drug + co-solvent = 10 mg + 259.47 mg).

Determination of the weight of carrier material

The weight of the liquid drug (W) was 269.47 mg, and the liquid load factor (Lf) was 1.5. These figures were utilized to compute the weight of the carrying material. It was determined that the carrier substance weighed 11.31 mg.

Primary trial for selection of carrier and coating material

Table 3 provides the batch of liquisolid compact composition. According to the mathematical processes explained in the above section, the amount of maisine, the carrier material, and the coating substance has been determined. The formulation also included magnesium stearate (MgS) as a lubricant (1% w/w), and sodium carboxymethyl cellulose as a disintegrant (4% w/w). The ratio of neusilin/corn starch, as well as the R-value (carrier/coating material), were found to have an essential impact on the release of drug by the liquisolid compact during preliminary trials, so it has been decided to utilize 3^2 full factorial designs to determine how much of an impact they had on the anticipated characteristics of the product. The transformed as well as coded values of variables and outcomes obtained are shown in Table 3.

Table 3. Composition of design batches for SGN liquisolid Tablet.

CODE	SGN	Maisine	Neusilin + Corn Starch	Aerosil 200	Sodium CMC (4%)	MgS (1%)	Total Weight
SLT -1	10	259.47	169.65 (152.69 + 16.96)	33.93	18.92	4.92	496.89
SLT - 2	10	259.47	169.65 (135.72+33.93)	33.93	18.92	4.92	496.89
SLT -3	10	259.47	169.65 (118.76+50.89)	33.93	18.92	4.92	496.89
SLT -4	10	259.47	169.65 (152.69 + 16.96)	22.62	18.92	4.92	485.58
SLT -5	10	259.47	169.65 (135.72+33.93)	22.62	18.92	4.92	485.58
SLT -6	10	259.47	169.65 (118.76+50.89)	22.62	18.92	4.92	485.58
SLT -7	10	259.47	169.65 (152.69 + 16.96)	11.31	18.92	4.92	474.27
SLT -8	10	259.47	169.65 (135.72+33.93)	11.31	18.92	4.92	474.27
SLT -9	10	259.47	169.65 (118.76+50.89)	11.31	18.92	4.92	474.27

* **All the weights are in mg**

Preparation of SGN liquisolid tablet

Fitting of data into the model

Using Design-Expert software, all the observed responses collected for 9 formulations have been simultaneously fitted into various mathematical models to choose the model that provides the best results. Multiple correlation coefficients (R^2) high values, adjusted R^2 values, anticipated R^2 values, coefficients of variation (%CV), and PRESS (Predicted Residual Sums of the Square) were used to determine which model was the best match (Table 4). The PRESS value of the model shows how well it fits the data. The chosen model should have a low PRESS value as compared to the other models.

Table 4. Regression analysis results obtained for various responses Y_1 (% drug release) and and Y_2 (disintegration time time) of SGN-LST for fitting to different models.

Models	SD	R^2	Adjusted R^2	Predicted R^2	PRESS	CV (%)	Remark
Response (Y_1)							
Linear	7.58	0.6760	0.5680	0.3293	713.00	9.17	
2FI	8.24	0.6804	0.4886	-0.1896	1264.68	9.98	
Quadratic	2.51	0.9823	0.9527	0.7861	227.43	3.04	Suggested
Response (Y_2)							
Linear	2.14	0.9584	0.9446	0.9058	62.47	3.35	
2FI	2.34	0.9588	0.9341	0.8078	127.40	3.66	
Quadratic	1.27	0.9927	0.9804	0.9156	55.96	1.99	Suggested

SD: standard deviation, R^2: multiple correlation coefficient, 2FI: two factor interaction, PRESS: predicted residual sum of square, CV: coefficient of variation.

Effect of independent variables on Y_1

Table 1 displays the SGN-LST formulations' percent drug release. The percentage release of drug values has been discovered in the ranges of 63.43±4.32% to 98.76±2.88%. This quadratic equation may be used to explain how the independent variables affect the percent drug release.

$$Y_1 = + 91.18 + 5.60\ X_1 + 9.41X_2 - 1.08X_1X_2 - 0.23X_1^2 - 12.66X_2^2 \quad (11)$$

The formula demonstrates that the neusilin: Corn starch ratio (X2) and the carrier: coating ratio (X^1) have a favorable impact on the Y^1. The X^2 obtains a high coefficient value, indicating that its influence on Y1 is greater than that of X^1. The ANOVA outcomes for the percent medication release data are provided in Table 5. The F-value of 33.21 for the model suggests that it is significant. In this study, X_1, X_2, and X_2^2 exhibited significant effects on Y_1. The adjusted R^2 of 0.9527 and the predicted R^2 of 0.7861 agree on reasonable terms. A suitable precision ratio of 16.772 suggests a sufficient signal. Consequently, it is possible to navigate the space of design using the quadratic model (Table 4). The 3-D response surface graphs (Figure 1A) and their related plots of 2-D Contour plots (Figure 1B) show the influence of the independent factors on Y_1. 3D plot and its perturbation plot show that the increase in carrier concentration: neusilin and coating ratio: corn starch ratio drug release increases. These data were also confirmed by the percent drug release perturbation plot (Figure 1C). The graph of perturbation shows a little bend for factor X_1 and a steeper incline for factor X_2, confirming the prominent effect of X_2 on percent drug release [43].

Table 5. ANOVA results for various responses of SGN-LTS Tablet.

Source	Responses					
	Y_1 (% drug release)			Y_2 (disintegration time)		
	F-value	p-value Prob > F	Adequacy precision	F-value	p-value Prob > F	Adequacy precision
Model	33.21	0.0079	16.772	69.17	< 0.0001	22.091
X_1	29.89	0.0120		24.53	0.0026	
X_2	84.40	0.0027		113.81	< 0.0001	
X_1X_2	0.74	0.4533				
X_1^2	0.017	0.9050				
X_2^2	51.01	0.0057				

X_1, and X_2 are coded terms for independent variables; X_1X_2 interaction terms; X_1^2 and X_2^2 are quadratic terms

Effect of independent variables on disintegration time (Y_2) of SGN-LST

Table 1 displays the findings of the SGN-LST formulations' disintegration times. The Y_2 has been discovered to be ranging from 52.82±1.72 to 78.12±6.54 sec. The following linear equation may be used to show how the independent variables affect Y_2.

$$Y_2 = + 63.89 - 4.33\ X_1 - 9.33\ X_2 \quad (12)$$

The disintegration time is negatively impacted by both the independent variables. This illustrates that the SGN-LST disintegration time reduces as increases "carrier: coating ratio (X_1) and neusilin: Corn starch ratio (X_2). According to the X_2 high coefficient value, X_2 has" a more significant impact on the time of disintegration of the SGN-LST than that of X_1. Table 5 displays the ANOVA findings for the Y_2 data. The model is significant, revealed by the F-value of 69.17. In this example, the model terms X_1 and X_2 are important. The anticipated R^2 of 0.9058 and the adjusted R^2 of 0.9446 are reasonably in agreement. An appropriate "signal is indicated by the adequate precision ratio of 22.091 (Table 4). As a consequence, the design space may be explored using the linear model. Figure 1D and Figure 1E show 3-D response surface and 2-D contour plots, respectively, that" show how independent variables affect the time of disintegration. The impact of separate variables on responses may also be understood through a perturbation plot. The findings of the graphs of the 3-D response surface and the plots of the 2-D contour were also corroborated by the perturbation plot (Figure 1F) for the disintegration time. Linear lines in the perturbation plot reveal the linear effect of the independent variable on Y_2. Numerical optimization was conducted by imposing constraints on the independent variables (Y_1-maximize; and Y_2-minimize) to identify the optimum formulation of SGN-LST in the space of design. The optimized formulation (desirability: 0.945) and its expected response values are shown in the overlay plot (Figure 1G). The developed and analyzed SGN-LST formulation was optimized for the responses. Table 6 displays the optimized formulation's expected and measured response values, together with corresponding predicted error percentages. The values' strong agreement served as evidence of the validity and optimization of the design. The percent prediction error values have been in a reasonable range, validating the model utilized for SGN-LTS optimization.

Table 6. Validation of optimized formulation.

Response	Predicted value	Observed value	Prediction error (%)
% Drug release	95.29	98.21	-2.92
Disintegration time (sec)	52.24	51.37	0.87

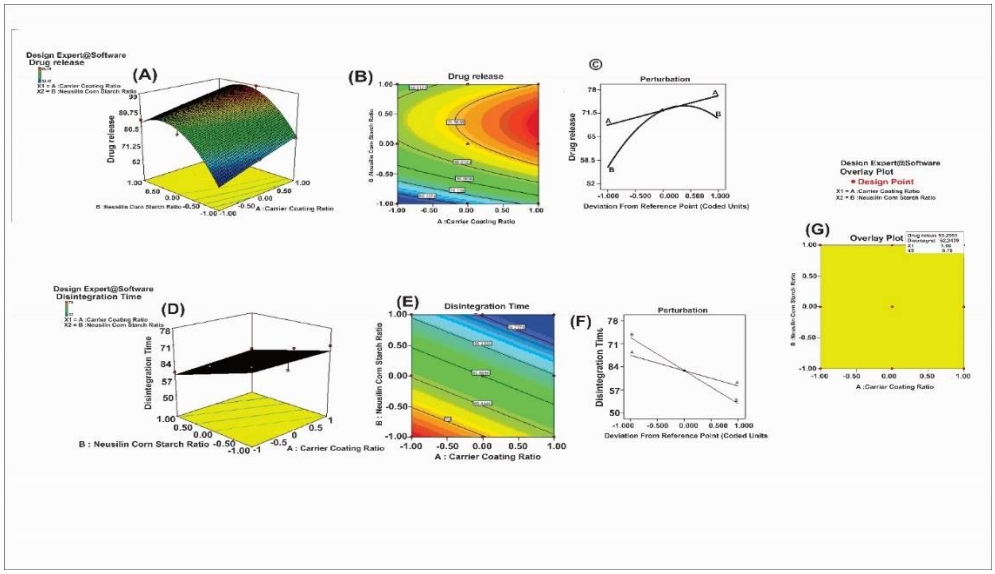

Figure 1. 3D-Response surface (A), 2D-contour (B) and perturbation plots (C) showing the effect of carrier: coating ratio and neusilin: corn starch ratio on % drug release of SGN-LST. D) 3D-Response surface (A), 2D-contour € and perturbation plots (F) showing the effect of carrier: coating ratio and neusilin: corn starch ratio on disintegration time of SGN-LST. G) The overlay plot displaying the optimized SGN-LST formulation in the design space and their predicted response values.

Micromeritic properties of optimized SGN liquisolid tablet

The SGN-LST 6 formulation's angle of repose was 29.93±0.266°, suggesting strong flow characteristics. The results showed that BD and TD were, respectively, 0.3963±0.030g/mL and 0.4100±0.022g/mL. While the HR was 1.034±0.062, the CCI was found to be 3.34±0.15%.

Post-compression evaluation

The optimized SGN liquisolid tablet (SGN-LST 6) was found to have the features that follow: drug content, hardness, friability, and weight variation: 99.31±2.1%, 2.9±0.83 kg/cm2, 0.33±0.018%, and 484.48±1.32 mg, respectively. Detailed results are shown in Table 7.

Table 7. Drug content, Hardness, Friability and Weight Variation of SGN liquisolid Tablet.

CODE	Drug content (%)	Hardness kg/cm^2	(%) Friability	Weight variation (mg±%)
SLT -1	78.24±2.8	2.5±0.26	0.48±0.032	496.89±1.48
SLT - 2	85.54±2.4	2.8±0.35	0.40±0.029	496.89±1.65
SLT -3	87.81±2.6	2.6±0.75	0.43±0.044	496.89±1.19
SLT -4	93.14±3.4	2.9±0.83	0.37±0.037	485.58±1.37
SLT -5	94.54±3.8	3.1±0.87	0.31±0.027	485.58±1.54
SLT -6	99.31±2.5	3.0±0.54	0.33±0.018	484.48±1.32
SLT -7	86.74±3.8	2.7±0.48	0.41±0.051	474.27±1.84
SLT -8	87.64±3.8	3.2±0.79	0.26±0.027	474.27±1.72
SLT -9	91.25±2.9	3.1±0.61	0.30±0.057	474.27±1.61

Drug-excipients compatibility study

FTIR

FTIR spectrum analysis had been utilized to investigate the compatibility between the SGN and excipients of the liquid-solid system**.** Figure 2 displays "the FTIR spectra of pure SGN, maisine, neusilin-US2, and a physical mixture of the excipients used to make SGN liquisolid tablets. FTIR spectra of SGN (Figure 2A), showed stretching =C-H at 3479.23 cm^{-1}, aromatic C-H at 3111.93cm^{-1} C-H aliphatic at 2929.10cm^{-1}, C=O stretch at 1740.19cm^{-1}, C=O-NH stretching" at 1660.49cm^{-1}, amines at 1501.37cm^{-1} 1432.82cm^{-1}, S=O stretch at 1051.83cm^{-1} and -C-S stretch at 790.02cm^{-1}, respectively. The outcomes correspond with the earlier Rasul et al. report.[44] Figure 2B and Figure 2C display the FTIR spectrum of Maisine and Neusilin, respectively. The FTIR spectrum of SGN-LST (Figure 2D), showed stretching =C-H "at 3445.15cm^{-1}, aromatic C-H at 3132.91cm^{-1} C-H aliphatic at 2912.87cm^{-1}, C=O stretch at 1758.61cm^{-1}, C=O-NH stretching at 1631.29cm^{-1}, amines at" 1513.31cm^{-1} 1467.21cm^{-1}, S=O stretch at 1027.36cm^{-1} and -C-S stretch at 773.70cm^{-1}, respectively. The FTIR spectra of SGN-LST retain the primary SGN peaks. The results demonstrated compatibility because there was no chemical interaction between SGN and the SGN-LST formulation excipients [45].

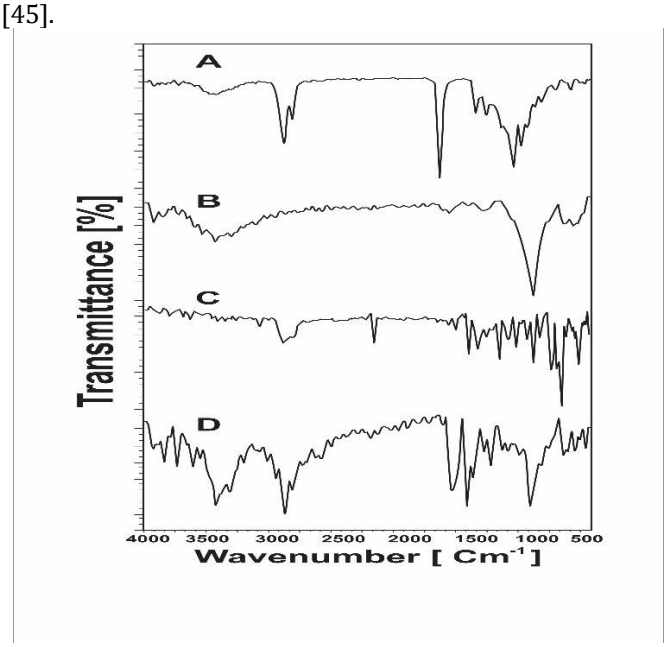

Figure 2. FTIR spectra of A) SGN B) Maisine C) Neusilin and D) SGN-LST Tablet.

DSC Studies.

The DSC analysis was conducted to evaluate the samples' crystallinity and melting behavior. Figure 3 displays the DSC thermograms of SGN-LST, maisine, neusilin, and plain SGN. Neusilin-US2 (Figure 3B) displayed peaks at 202.56°C, which corresponds to the peak of neusilin, while the DSC thermogram of plain SGN (Figure 3A) exhibited peaks matching to SGN at 100.77°C. Conversely, an endothermic peak corresponding to neusilin has been observed at 206.12°C in the DSC thermogram of SGN-LST (Figure 3C).

It also indicates that the SGN included in the liquisolid compact was present in a non-crystalline state, indicating that the SGN may have become molecularly distributed or transformed into an amorphous state within the liquisolid compact. It also implies that SGN is entirely entrapped in the lipid matrix of the liquisolid compact [46].

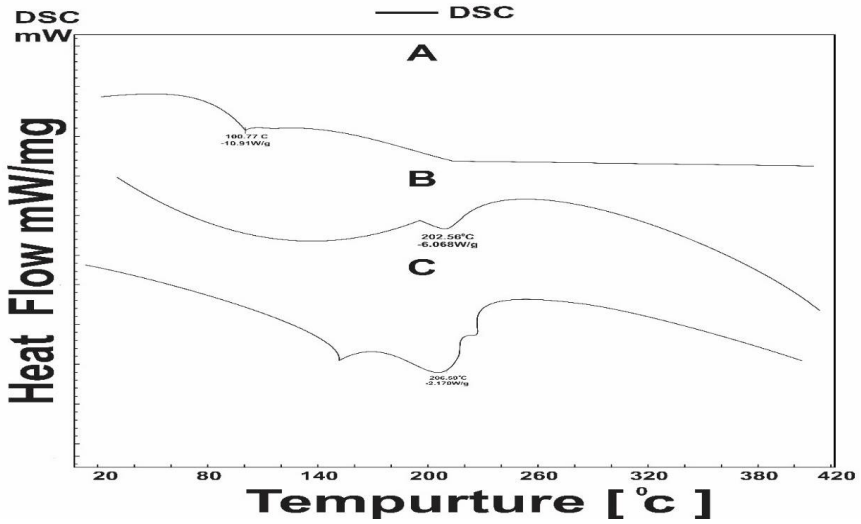

Figure 3. DSC thermogram of A) SGN B) Neusilin and C) SGN-LST Tablet.

P-XRD Studies.

The influence of process parameters of liquisolid compact preparation on the physicochemical nature of SGN was checked by P-XRD studies. XRD spectra of plain SGN and optimized SGN-LST are delineated in Figure 4. The P-XRD spectra of SGN (Figure. 4A) manifested specific intensity peaks counts of 117, 144, 162, 279, 306, 516, 664, 417, and 166 at diffraction angles of 6.82º, 11.03º, 13.63º, 19.99º, 20.03º, 20.02º, 20.11º and 24.53º (2θ), respectively, indicating its crystalline nature. Figure 4B displays FTIR spectra of Neusilin, indicating partial crystalline. However, these characteristic peaks disappeared in optimized SGN-LST (Figure 4C). This confirms that the crystalline state of SGN changes during the manufacturing process of liquisolid tablets. The acquired results are consistent with the "earlier publication [47].

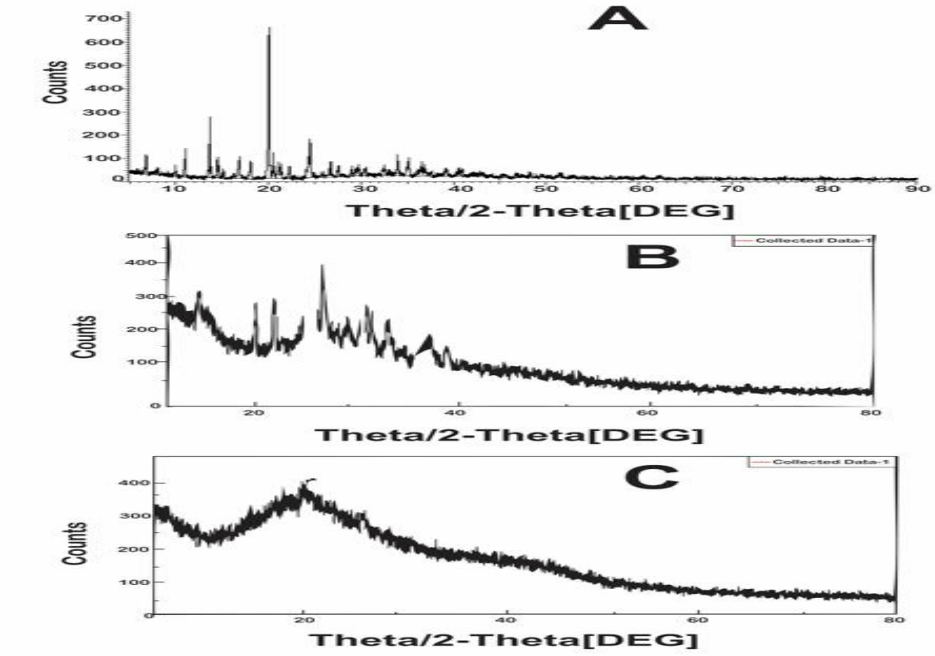

Figure 4. XRD diffractogram of A) SGN B) Neusilin and C) SGN-LST Tablet.

***In vitro* Antidiabetic Study.**

α-amylase Inhibitory Assay

α-amylase activity is measurable *in vitro* through the hydrolysis of starch in the existence of these enzymes. α-amylase, mostly" present in pancreatic juice and saliva, is considered one of the most important digestive enzymes since it plays a big part in breaking down polysaccharides. One potential method of preventing excessive postprandial blood glucose is to target and inhibit this enzyme [48]. Figure 5A illustrates the ability of SGN, SGN-LST, and acarbose to inhibit α-amylase. The IC_{50} value of 8.93±0.26 µg/mL "for SGN-LST and 7.65±0.33 µg/mL for normal acarbose indicate the two compounds have almost equal inhibitory potential. Conversely, SGN had an IC_{50} of 19.43±0.57 µg/mL. The reduced values of IC_{50} of SGN-LST indicate enhanced enzyme-induced hydrolysis of starch into monosaccharide, which is directly connected with the -amylase inhibitory" effect [48].

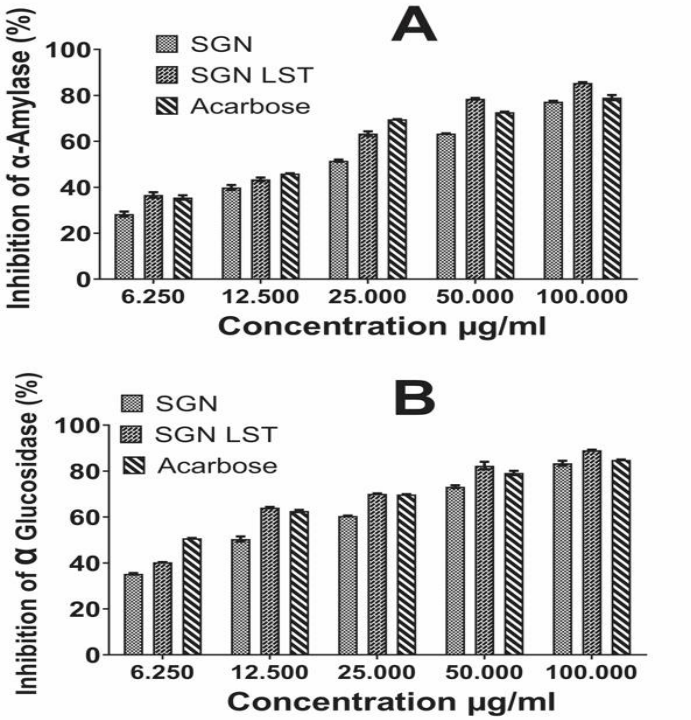

Figure 5. A) Alpha-amylase inhibition potential of SGN, SGN-LST and acarbose B) α-glucosidase inhibition of activity of SGN, SGN-LST and acarbose.

α-Glucosidase inhibition assays

α-glucosidase is another vital enzyme involved in the breakdown of carbohydrates which is found in the small intestine's mucosal brush boundary. In type 2 DM, delaying the absorption of glucose after a meal is a benefit of α-glucosidase inhibition medication. Blood glucose levels can be brought back to normal by blocking α-glucosidase, which may likely slow the progression of diabetes. Figure 5B demonstrates α-glucosidase inhibition activity of SGN, SGN-LST, and acarbose. According to the computed IC50 value, SGN-LST has a higher inhibitory potential (IC50: 7.92±0.18 µg/mL) than SGN, which has an IC_{50} of 26.11±0.27 µg/mL, which is comparable to normal acarbose (IC50: 6.57±0.14 µg/mL). The molecular dispersion of SGN in the lipid carriers of liquisolid compacts is primarily responsible for the enhanced antidiabetic potential [48].

***In Vivo* pharmacokinetic study**

It was discovered that SGN retained its plasma form for 2.8 min. The plasma conc. vs. time curves (Figure 6) shows that the C_{max} for pure SGN (59.27±8.62 ng/mL) was reached at 0.5 h (T_{max}), but the C_{max} for SGN-LST administration was reported to be 176.61±23.54 ng/mL, attained at 1 h. At every time point under investigation, the plasma concentration obtained following the administration of SGN-LST was considerably ($p<0.05$) higher than that of plain SGN. SGN-LST had an AUC that was significantly ($p<0.05$) greater than plain SGN (127.00±12.62 ng.h/mL), at 506.74±42.78 ng.h/mL. The half-lives (T1/2) for SGN-LST and SGN elimination were calculated to be 3.34±0.31 h and 1.56±0.13 h, respectively. The results indicated that the Mean Residence Times (MRT) for SGN-LST and SGN were 2.44±0.18 h and 4.15±0.32 h, respectively [49]. Table 8 displays comprehensive results. A remarkable 4-fold increase in bioavailability

as compared to plain SGN is primarily attributable to enhanced dissolution rate, which primarily entails a rise in wettability, solubility, and surface area [50-54].

Table 8. Pharmacokinetic Parameters of Sexagliptin (SGN) after oral administration of SGN and SGN-LST formulation (5 mg/kg) in rats.

Parameter	SGN	SGN-LST
T_{max} (h)	0.5	1
C_{max} (ng/ml)	59.27±8.62	176.61±23.54
AUC (ng/ml*h)	127.00±12.62	506.74±42.78
AUMC (ng/ml*h^2)	313.69±22.51	2134.36±53.87
t1/2 (h)	1.56±0.13	3.34±0.31
MRT (h)	2.44±0.18	4.15±0.32
CL (mg)/(ng/ml)/h	0.038	0.009
Relative Bioavailability		399.00

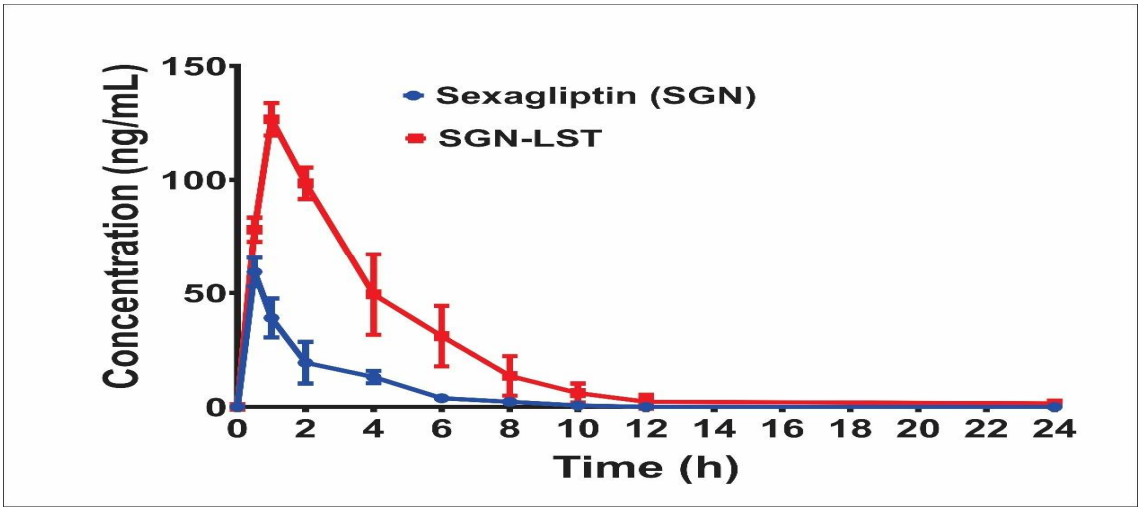

Figure 6. In-vivo Pharmacokinetic study of SGN and SGN-LST after 24 hours in albino wistar rats.

Stability study

To determine the impact of "storage conditions on cumulative drug release and optimized SGN-LST disintegration time, a stability" study was conducted for three months at accelerated RH and temperature (40±2°C and 75±5%). After three months of storage, there were no discernible changes ($p>0.05$) in the percentage drug release and disintegration time of the liquisolid tablet (Table 9), indicating a high degree of stability.

Table 9. Accelerated Stability Study Data of SGN Liquisolid Tablet for 03 Months period.

Parameter	Initial	1 Month	2 Month	3 Month
CDR (%)	99.08±0.24	98.83±0.29	98.74±0.37	98.25±0.46
Disintegration Time (Sec.)	57.32±1.23	56.54±1.50	56.34 ±2.13	55.0±2.54

All values represent mean ± standard deviation (n=3)

DISCUSSION

Diabetes mellitus, characterized by dysregulated blood glucose levels, imposes a significant global health burden, underscoring the urgency for novel therapeutic interventions. Traditional drug delivery systems often encounter limitations in terms of drug solubility, bioavailability, and pharmacokinetic profiles, necessitating the exploration of alternative formulations. By leveraging advanced formulation techniques such as liquisolid technology, which enhances drug solubility and bioavailability, the study endeavors to bridge existing gaps in diabetes treatment. The undertaking of this study underscores the critical need for innovative approaches in pharmaceutical research to address the escalating challenges posed by chronic diseases such as diabetes.

The research carried out a comprehensive study on the development and optimization of SGN liquisolid tablets (SGN-LST) for diabetes treatment. The experiments revealed important results that helped expose the properties of the formulation, its ability to inhibit glucose metabolism's enzymes, pharmacokinetic profile, and stability. To decide on the best lipid vehicle for SGN, solubility studies were conducted with maisine found to be highly suitable as compared to the others. Neusilin was preferred as carrier material due to its high flow liquid retention capacity while maize starch was included in order to enhance the

release of drug from the neusilin matrix. The ratio of carrier materials and coating materials was optimized after mathematical modeling using factorial design and consequently resulted in several SGN-LST formulations. In rats' *in-vivo* studies, plain SGN LST showed 4-fold increases in bioavailability over SGN alone indicating better bioavailability than plain drug. An antidiabetic potential was indicated by findings showing that SGN-LST could inhibit α-amylase and α-glucosidase enzymes involved in carbohydrate metabolism through *in vitro* assays.

FTIR spectroscopy and DSC analysis during compatibility studies showed the absence of any chemical interaction between SGN and the excipients thereby confirming formulation compatibility.[46] The p-XRD results indicated that there was an amorphous to crystalline transition in the liquisolid compact for SGN, which consequently led to improved dissolution properties.[47] The optimized SGN-LST formulation had good stability as shown by stability studies conducted over three months under accelerated conditions which did not show significant changes in drug release or disintegration time. SGN-LST was found to have desirable characteristics for diabetes treatment such as bioavailability improvement, enzyme inhibition, and stability among others.[48] SGN-LST thus can be used as a carrier system for SGN, offering better performance in treating diabetics.

A higher dissolving rate has the potential to increase oral bioavailability and gastrointestinal absorption of the medication [55-56]. The drug is integrated "in a non-volatile solvent in a liquisolid compact, which enhances the dissolving rate by promoting wetting phenomena. By absorbing into or onto the carrier and coating material, the" medication is molecularly disseminated in the liquid vehicle. This increases the "surface area of the drug, facilitating faster wetting and dissolving of the drug and exhibiting higher oral bioavailability [57-59]. The bio-adhesive characteristics of lipids help liquisolid compacts stick to the apical membrane, increasing residence time and, consequently, absorption as well as bioavailability [60-63]. The research" therefore is a collective effort on development and evaluation of SGN-LST and its prospects on diabetes management. It may be necessary to carry out further investigations on its effectiveness and safety in clinical settings involving humans.

CONCLUSION

In the current study, a factorial design was employed to successfully develop and optimize SGN-LST. The optimized SGN-LST was assessed for a range of *in vitro* and *in vivo* characteristics. The flow characteristics, compactability, hardness, friability, content homogeneity, and disintegration time were found to be considerable. At all the specified time intervals, the release of the drug from SGN-LST was noticeably higher in comparison to the plain SGN. The SGN was either in an amorphous condition or was molecularly dispersed in the liquisolid tablet, according to the DSC and XRD data, which indicated an enhanced dissolution profile of the liquisolid compact. The α-amylase inhibition and α-glucosidase inhibition assay demonstrated remarkable anti-diabetic effectiveness of SGN-LST than plain SGN *in vitro*. Further, an *in vivo* pharmacokinetic study in rats revealed substantial enhancement in the bioavailability of SGN from SGN-LST than plain SGN. In a nutshell, SGN's liquisolid compact could be a potential way for SGN delivery with improved therapeutic performance in the treatment of diabetes. Saxagliptin (SGN)-loaded liquid-solid tablet (LST) for improved diabetes treatment. Optimized formulation (SGN-SLT-6) quickly disintegrates with high drug release. SGN-LST showed a 4-fold bioavailability than plain SGN when orally administered to rats. LST markedly enhanced SGN's *in vitro* and *in vivo* effectiveness in treating diabetes. LST is a promising delivery vehicle for effective SGN management in diabetes.

DECLARATIONS

ETHICS APPROVAL AND CONSENT TO PARTICIPATE

Applicable

CONSENT FOR PUBLICATION

Not applicable

AVAILABILITY OF DATA AND MATERIAL

Applicable

COMPETING INTEREST

The authors declare that they have no competing interests.

FUNDING

No funding was received for this project.

ACKNOWLEDGEMENT
The authors are thankful to Vels Institute of Science, Technology and Advanced Studies (VISTAS), Pallvaram, Chennai-600112 for providing required guidance and support for completion of present research work. Authors are also thankful to department of pharmaceutics Vasantidevi Patil Institute of Pharmacy, Kodoli-416114, Kolhapur, Maharashtra, India for providing required guidance and support. Authors are also thankful to Maratha Mandal Dental College and research center Belagavi for antidiabetic and in vivo bioavailability study and Diya labs Mumbai for analytical work.

ABBREVIATIONS
SGN- saxagliptin
SLT-1 to SLT-9- SGN liquisolid formulations
SGN-LST- saxagliptin-liquisolid tablets
Φ - number- flowable liquid-retention potential
Ψ - number- compressible liquid-retention potential

REFERENCES
1. Mobasseri M, Shi Mohammadi M, Amiri T, Vahed N, Hosseini Fard H, Ghojazadeh M, (2020). Prevalence and incidence of type 1 diabetes in the world: a systematic review and meta-analysis, Health Promot Perspec 10(2):98-115, doi: 10.34172/hpp.2020.18.
2. Divers J, Mayer-Davis EJ, Lawrence JM (2020).Trends in Incidence of Type 1 and Type 2 Diabetes Among Youths Selected Counties and Indian Reservations, United States, 2002–2015. MMWR Morb Mortal Wkly Rep 69(6):161–165.
3. Pradeepa, R, & Mohan, V (2021) Epidemiology of type 2 diabetes in India. Indian journal of ophthalmology 69 (11):2932.
4. Killedar SG, Nale AB, More HN, Nadaf SJ, Pawar AA, Tamboli US (2014) Isolation, characterization, and evaluation of Cassia fistula Linn. seed and pulp polymer for pharmaceutical application. Int J Pharm Investig 4(4): 215-5. doi: 10.4103/2230-973X.143128
5. Bonthagarala B, Dasari V, Kotra V, Swain S, Beg S (2019). Quality-by-Design based development and characterization of pioglitazone loaded liquisolid compact tablets with improved biopharmaceutical attributes. Journal of Drug Delivery Science and Technology 51:345-55.
6. Augeri DJ, Robl JA, Betebenner DA, Magnin DR, Khanna A, Robertson JG, Wang A, Simpkins LM, Taunk P, Huang Q, Han SP (2005). Discovery and preclinical profile of Saxagliptin (BMS-477118): a highly potent, long-acting, orally active dipeptidyl peptidase IV inhibitor for the treatment of type 2 diabetes. Journal of medicinal chemistry 48 (15): 5025-37.
7. Deepan T, Dhanaraju MD (2018). Stability indicating HPLC method for the simultaneous determination of dapagliflozin and saxagliptin in bulk and tablet dosage form. Current Issues in Pharmacy and Medical Sciences 31(1):39-43.
8. N. Singh, P. Bansal, M. Maithani (2018). Development and validation of a stability-indicating RP-HPLC method for simultaneous determination of dapagliflozin and saxagliptin in fixed-dose combination. New J. Chem 42:2459-2466.
9. W.L. Chiou, S (2007). Reiegelman, Pharmaceutical applications of solid dispersion systems, J. Pharm. Sci 60:281–1290.
10. N. Blagden, M. De Matas, P. Gavan, P. York (2007). Crystal engineering of active pharmaceutical ingredients to improve solubility and dissolution rates, Adv. Drug Deliv. Rev 59:617–630.
11. R. Sonoda, M. Horibe, T. Oshima (2008). Improvement of dissolution property of poorly water-soluble drugs by novel dry coating method using planetary ball mill, Chem. Pharm. Bull 56:1243–1247.
12. Jaydip B, Dhaval M, Soniwala MM, Chavda J (2020). Formulation and optimization of liquisolid compact for enhancing dissolution properties of efavirenz by using DoE approach. Saudi Pharm J 28(6):737-745. doi: 10.1016/j.jsps.2020.04.016.
13. Chella N, Narra N, Rama Rao T (2014). Preparation and characterization of liquisolid compacts for improved dissolution of telmisartan. Journal of drug delivery 1: 1-10.
14. Patel DS, Pipaliya RM, Surti N (2015) Liquisolid Tablets for Dissolution Enhancement of a Hypolipidemic Drug. Indian J Pharm Sci 77(3):290-8. doi: 10.4103/0250-474x.159618.
15. Patel H, Gupta N, Sonia P. Ranch, K (2019). Development of liquisolid tablets of chlorpromazine using 3^2 full factorial designs. Indian Journal of Pharmaceutical Sciences 81(6):1107-1114.
16. Cirri M, Mura P, Valleri M, Brunetti L (2020). Development and Characterization of Liquisolid Tablets Based on Mesoporous Clays or Silicas for Improving Glyburide Dissolution. Pharmaceutics 12:1-18. doi:503.https://doi.org/10.3390/pharmaceutics12060503.
17. Ahmed TA, Alotaibi HA, Alharbi WS, Safo MK, El-Say KM (2022). Development of 3D-Printed, Liquisolid and Directly Compressed Glimepiride Tablets, Loaded with Black Seed Oil Self-Nanoemulsifying Drug Delivery System: In Vitro and In Vivo Characterization. Pharmaceuticals (Basel) 15(68): 1-14, doi:

10.3390/ph15010068.
18. Vraníková B, Gajdziok J, Doležel P (2017). The effect of super disintegrants on the properties and dissolution profiles of liquisolid tablets containing rosuvastatin. Pharmaceutical development and technology 22(2):138-47.
19. Patel T, Patel LD, Suhagia BN, Soni T, Patel T (2014). Formulation of fenofibrate liquisolid tablets using central composite design. Curr Drug Deliv 11(1):11-23, doi: 10.2174/15672018113109990051.
20. Galatage ST, Trivedi R, Bhagwat DA (2022). Oral self-emulsifying nanoemulsion systems for enhancing dissolution, bioavailability and anticancer effects of camptothecin. Journal of Drug Delivery Science and Technology 78:103929, https://doi.org/10.1016/j.jddst.2022.103929.
21. Spireas S, Sadu S, Grover R (1998). In vitro. release evaluation of hydrocortisone liquisolid tablets, J Pharm Sci 87:867-872.
22. Elkordy AA, Tan XN, Essa EA (2013). Spironolactone release from liquisolid formulations prepared with Capryol™ 90, Solutol® HS-15 and Kollicoat® SR 30 D as non-volatile liquid vehicles. European journal of pharmaceutics and biopharmaceutics 83(2):203-23.
23. Javadzadeh Y, Jafari-Navimipour B, Nokhodchi A (2007) Liquisolid technique for dissolution rate enhancement of a high dose water-insoluble drug (carbamazepine). International journal of pharmaceutics 341 (1):26-34.
24. S. Nazzal, M.Nutan, A. Palamakula, R. Shah, A. Zaghloul, M. Khan (2022) Optimization of a self-nanoemulsified tablet dosage form of Ubiquinone using response surface methodology: Effect of Formulation Ingredients, Int. J. Pharm 240:103–114.
25. Kumbar VM, Muddapur U, Bin Muhsinah A, Alshehri SA, Alshahrani MM, Almazni IA, Kugaji MS, Bhat K, Peram MR (2022). Curcumin-Encapsulated Nanomicelles Improve Cellular Uptake and Cytotoxicity in Cisplatin-Resistant Human Oral Cancer Cells. J Funct Biomater 13(4):158. doi: 10.3390/jfb13040158.
26. G A. A. Gerencser, C.Chinopoulos, M.J. Birket, M. Jastroch, C.Vitelli, D.G. Nicholls, M.D.Brand (2012). Quantitative measurement of mitochondrial membrane potential in cultured cells, calcium-induced de- and hyperpolarization of neuronal mitochondria, J Physiol 1:2845-71.
27. Gurav S, Usapkar P, Gurav N, Nadaf S, Ayyanar M, Verekar R, Bhole R, Venkataramaiah C, Jena G, Chikhale R (2022). Preparation, characterization, and evaluation (in-vitro, ex-vivo, and in-vivo) of naturosomal nanocarriers for enhanced delivery and therapeutic efficacy of hesperetin. Plos one 17(11): e0274916.
28. Bhagwat DA, Swami PA, Nadaf SJ, Choudhari PB, Kumbar VM, More HN, Killedar SG, Kawtikwar PS (2021). Capsaicin loaded solid SNEDDS for enhanced bioavailability and anticancer activity: in-vitro, in-silico, and in-vivo characterization. Journal of Pharmaceutical Sciences 110 (1):280-91.
29. G.M.Morris, H. Ruth, W. Lindstrom, M.F. Sanner, R.K. Belew, D.S. Goodsell, A.J. Olson (2006) Software news and updates AutoDock4 and AutoDockTools4: Automated docking with selective receptor flexibility, J. Comput. Chem 30:2785–2791.
30. Kumbhar BV, Bhandare VV (2021). Exploring the interaction of Peloruside-A with drug resistant αβII and αβIII tubulin isotypes in human ovarian carcinoma using a molecular modeling approach. Journal of Biomolecular Structure and Dynamics 39(6):1990-2002.
31. Kumbhar BV, Bhandare VV, Panda D, Kunwar A (2019). Delineating the interaction of combretastatin A-4 with αβ tubulin isotypes present in drug resistant human lung carcinoma using a molecular modeling approach. Journal of biomolecular structure and Dynamics 8(2):426-438, doi: 10.1080/07391102.2019.1577174.
32. Rai, Gupta, T.K, Kini, S.A. Kunwar, A. Surolia, D. Panda (2013). CXI-benzo-84 reversibly binds to tubulin at colchicine site and induces apoptosis in cancer cells, Biochem. Pharmacol 86:378–391.
33. Venghateri JB, Gupta TK, Verma PJ, Kunwar A, Panda D (2013). Ansamitocin P3 depolymerizes microtubules and induces apoptosis by binding to tubulin at the vinblastine site. PloS one 8(10): e75182.
34. W. L. DeLano, The PyMOL Molecular Graphics System, Schrödinger LLC (2003).
35. Patil SM, Choudhari AU (2018) Development of UV Spectrophotometric Method for Estimation of Letrozole in Pure and Pharmaceutical Dosage Form. Indo American Journal of Pharmaceutical Research 8 (04):1080-1085.
36. Nadaf S, Desai R, More T, Shinde P, Dakare S, Killedar S (2020) Antiproliferative and caspase-mediated apoptosis inducing effects of Murraya koenigii seeds against cancer cells. South African Journal of Botany 132:328-37.
37. Kim KY, Nam KA, Kurihara H, Kim SM (2008) Potent α-glucosidase inhibitors purified from the red alga Grateloupia elliptica. Phytochemistry 69 (16):2820-5.
38. L. H. Bosenberg and D. G. Van Zyl (2008) The mechanism of action of oral antidiabetic drugs: a review of recent literature, Journal of Endocrinology, Metabolism and Diabetes of South Africa 13(3):80–88.
39. Peram MR, Jalalpure S, Kumbar V, Patil S, Joshi S, Bhat K, Diwan P (2019) Factorial design-based curcumin ethosomal nanocarriers for the skin cancer delivery: in vitro evaluation. Journal of liposome research 29(3):291-311.
40. Kottke MK, Chueh HR, Rhodes CT (1992). Comparison of disintegrant and binder activity of three corn starch products. Drug development and industrial pharmacy 18(20):2207-23.
41. Spireas S, Sadu S (1998) Enhancement of prednisolone dissolution properties using liquisolid compacts. International Journal of Pharmaceutics 166(2):177-88.

42. Zhao H, Shi C, Zhao L, Wang Y, Shen L (2022). Influences of different microcrystalline cellulose (MCC) grades on tablet quality and compression behavior of MCC-lactose binary mixtures. Journal of Drug Delivery Science and Technology 77:103893.
43. Rasul A, Maheen S, Khan HU, Rasool M, Shah S, Abbas G, Afzal K, Tariq F, Shahzadi I, Asad MH (2021) Formulation, Optimization, In Vitro and In Vivo Evaluation of Saxagliptin-Loaded Lipospheres for an Improved Pharmacokinetic Behavior. BioMed Research International 20: 1-7. https://doi.org/10.1155/2021/3849093.
44. Alhamhoom Y, Ravi G, Osmani RA, Hani U, Prakash GM (2022). Formulation, characterization, and evaluation of eudragit-coated saxagliptin nanoparticles using 3 factorial design modules. Molecules 27(21):7510. doi: 10.3390/molecules27217510.
45. Dhere MD, Bhavya E (2022). Design and Characterization of Barberine Liquisolid Compacts For Escalating Bioavailability And Antidiabetic Potential: In Vitro, In Vivo And In Silico Approach. Journal of Pharmaceutical Negative Results 1: 9394-414.
46. Patil MP, Jin X, Simeon NC, Palma J, Kim D, Ngabire D, Kim NH, Tarte NH, Kim GD (2018) Anticancer activity of Sasa borealis leaf extract-mediated gold nanoparticles. Artificial cells, nanomedicine, and biotechnology 46(1):82-8.
47. Ting L, Zhang XD, Song YW, Lui JW (2006). A microplate-based screening method for alpha-glucosidase inhibitors. Chinese Journal of Clinical Pharmacology and Therapeutics 10(10):1128.
48. Kodoli RS, Killedar SG, Pishwikar SA, Habbu PV, Bhagwat DA (2021). Hepatoprotective activity of Phyllanthus niruri Linn. endophytes. Future Journal of Pharmaceutical Sciences 7(97):1-13. https://doi.org/10.1186/s43094-021-00243-1.
49. Rasul A, Maheen S, Khan HU, Rasool M, Shah S, Abbas G, Afzal K, Tariq F, Shahzadi I, Asad MH (2021). Formulation, Optimization, In Vitro and In Vivo Evaluation of Saxagliptin-Loaded Lipospheres for an Improved Pharmacokinetic Behavior. BioMed Research International 1-7.doi: 10.1155/2021/3849093.
50. Javadzadeh Y, Siahi-Shadbad MR, Barzegar-Jalali M, Nokhodchi A (2005). Enhancement of dissolution rate of piroxicam using liquisolid compacts. Il Farmaco 60(4):361-5.
51. Javadzadeh Y, Siahi MR, Asnaashari S, Nokhodchi A (2007). An investigation of physicochemical properties of piroxicam liquisolid compacts. Pharmaceutical development and technology 12(3):337-43.
52. Nokhodchi A, Javadzadeh Y, Siahi-Shadbad MR, Barzegar-Jalali M (2005). The effect of type and concentration of vehicles on the dissolution rate of a poorly soluble drug (indomethacin) from liquisolid compacts. J Pharm Pharm Sci 8(1):18-25.
53. Yadav VB, Yadav AV (2009). Improvement of solubility and dissolution of indomethacin by liquisolid and compaction granulation technique. Journal of pharmaceutical sciences and research 1 (13):44-51.
54. Karmarkar A, Gonjari I, Hosman A, Dhabal P, Bhis S (2009). Liquisolid tablets: a novel approach for drug delivery. International Journal of Health Research 2(1):45-50.
55. Nokhodchi A, Hentzschel CM, Leopold CS (2011). Drug release from liquisolid systems: speed it up, slow it down. Expert opinion on drug delivery 8(2):191-205.
56. El-Houssieny BM, Wahman L, Arafa N (2010). Bioavailability and biological activity of liquisolid compact formula of repaglinide and its effect on glucose tolerance in rabbits. Bioscience trends 4(1):17-24.
57. Khaled KA, Asiri YA, El-Sayed YM (2001). In vivo evaluation of hydrochlorothiazide liquisolid tablets in beagle dogs. International journal of pharmaceutics 222 (1):1-6.
58. Raval C, Joshi N, Patel J, Upadhyay UM (2012) Enhanced oral bioavailability of olmesartan by using novel solid self-emulsifying drug delivery system. Int J Adv Pharm 2:82-92.
59. Nepal PR, Han HK, Choi HK (2010). Preparation and in vitro–in vivo evaluation of Witepsol H35 based self-nanoemulsifying drug delivery systems (SNEDDS) of coenzyme Q10. Eur J Pharm Sci 39:224-232.
60. Galatage ST, Manjappa AS, Bhagwat DA, Trivedi R, Salawi A, Sabei FY, Alsalhi A (2023). Oral self-nanoemulsifying drug delivery systems for enhancing bioavailability and anticancer potential of fosfestrol: In vitro and In vivo characterization. Eur J Pharm Biopharm 17:S0939-6411(23)00273-4. doi: 10.1016/j.ejpb.2023.10.013.
61. Shaya JA, Afzal H, Mohammad Y (2022) Impact of composition and morphology of ketoconazole-loaded solid lipid nanoparticles on intestinal permeation and gastroplus based prediction studies. ACS Omega, 7:2406– 22420.
62. Patil, K. S., Hajare, A. A., Manjappa, A. S., More, H. N., & Disouza, J. I. (2021). Design, development, in silico and in vitro characterization of Docetaxel-loaded TPGS/Pluronic F 108 mixed micelles for improved cancer treatment. Journal of Drug Delivery Science and Technology, 65, 102685.
63. Sambamoorthy, U, Manjappa AS, Eswara BR. M., Sanapala, AK., & Nagadeepthi, N. (2022). Vitamin E oil incorporated liposomal melphalan and simvastatin: approach to obtain improved physicochemical characteristics of hydrolysable melphalan and anticancer activity in combination with simvastatin against multiple myeloma. AAPS Pharm Sci Tech, 23, 1-16.